Algal Research 54 (2021) 102176

Contents lists available at ScienceDirect

Algal Research

journal homepage: www.elsevier.com/locate/algal

Photosynthetic performance of *Chlorella vulgaris* R117 mass culture is moderated by diurnal oxygen gradients in an outdoor thin layer cascade

Tomás Agustín Rearte [a,b,*], Paula S.M. Celis-Plá [c,d], Amir Neori [e,f], Jiří Masojídek [g,h], Giuseppe Torzillo [i,k], Cintia Gómez-Serrano [j], Ana Margarita Silva Benavides [k], Félix Álvarez-Gómez [l], R.T. Abdala-Díaz [l], Karolína Ranglová [g,m], Martín Caporgno [g], Thaís Fávero Massocato [n], Jaqueline Carmo da Silva [o], Hafidh Al Mahrouqui [j,p], Richard Atzmüller [q], Félix L. Figueroa [l]

[a] *Departamento de Recursos Naturales y Ambiente, Facultad de Agronomía, Universidad de Buenos Aires, CABA, Av. San Martín 4453, 1417 Buenos Aires, Argentina*
[b] *Consejo Nacional de Investigaciones Científicas y Tecnológicas (CONICET), Argentina*
[c] *Laboratory of Coastal Environmental Research, Center of Advanced Studies, University of Playa Ancha, Viña del Mar, Chile*
[d] *HUB-AMBIENTAL UPLA, Vicerrectoría de Investigación Postgrado e Innovación, Universidad de Playa Ancha, Valparaíso 2340000, Chile*
[e] *Morris Kahn Marine Research Station, Marine Biology Department, The Leon H. Charney School of Marine Sciences, University of Haifa, Israel*
[f] *The Interuniversity Institute for Marine Sciences, Eilat, Israel*
[g] *Centre Algatech, Institute of Microbiology, Czech Academy of Sciences, Třeboň, Czech Republic*
[h] *Faculty of Science, University of South Bohemia, České Budějovice, Czech Republic*
[i] *Institute of Bioeconomy, Department of Biology Agriculture and Food Sciences, CNR, Via Madonna del Piano, 10, I-50019 Sesto Fiorentino, Florence, Italy*
[j] *Department of Chemical Engineering, University of Almeria, Almería, Spain*
[k] *Escuela de Biología, CIMAR, Universidad de Costa Rica, San Pedro, de Montes de Oca, Costa Rica*
[l] *Malaga University, Research Institute for Blue biotechnology and development (IBYDA), San Julian, 2, 29008 Malaga, Spain*
[m] *Faculty of Agriculture, University of South Bohemia, České Budějovice, Czech Republic*
[n] *Botany Department, Center of Biological Sciences, Federal University of Santa Catarina, Santa Catarina, Brazil*
[o] *Department of Botany, Center of Biological Studies, Federal University of Sao Carlos, Sao Carlos, Brazil*
[p] *Sultan Qaboos University, Muscat, Oman*
[q] *FH OÖ Forschungs & Entwicklungs GmbH, Wels, Austria*

ARTICLE INFO

Keywords:
Chlorophyll fluorescence monitoring
Outdoor mass cultivation
PSII down-regulation
Oxygen production
Photoadaptation

ABSTRACT

Dissolved oxygen concentration is a critical point for microalgae in large scale cultivation systems. Highly productive cultures inevitably generate a build-up of oxygen gradients along the reactor which can affect photosynthetic performance. In this study, a fast-growing strain of *Chlorella vulgaris* R117 was cultured outdoors in a thin-layer cascade during a one-week trial reaching a biomass productivity of 4 g DW L^{-1} d^{-1} (27 g DW m^{-2} d^{-1}). High photosynthetic activity led to oxygen oversaturation of up to 400% in some parts along the culture units at midday. The aim was to examine the effect of high dissolved oxygen concentration on diurnal changes in the photosynthetic performance and growth of the *Chlorella* culture using multi-technique approach. Photosynthetic activity of *Chlorella R117* culture was estimated *in situ* and *ex situ* using oxygen production and *in vivo* Chl *a* fluorescence measurements, which showed good correlation. The rates of electron transport and of oxygen production were related, but the values of the $\mu mol_{electrons}/\mu molO_2$ ratio was higher than predicted, suggesting the probable involvement of electron and oxygen consuming processes such as photorespiration and Mehler reaction. These processes probably function as photoprotective mechanisms, since no photodamage was observed in the *Chlorella* R-117 cultures. Depression (down-regulation) of photosynthetic activity due to the exposition to high dissolved oxygen concentration along the cascade area over time was observed. The usefulness of *on-line* measurements was demonstrated to obtain immediate and *in-situ* information on the physiological status of the culture. This data can be used in models of operation control for large-scale microalgae production units.

* Corresponding author at: Consejo Nacional de Investigaciones Científicas y Tecnológicas (CONICET), Argentina.
E-mail address: tarearte@agro.uba.ar (T.A. Rearte).

https://doi.org/10.1016/j.algal.2020.102176
Received 30 March 2020; Received in revised form 16 December 2020; Accepted 16 December 2020
Available online 10 January 2021

1. Introduction

Shallow outdoor units for microalgae culturing were designed in the former Czechoslovakia during the 1950–1960s and used as one of the first large-scale microalgal culture systems in Europe [1]. The so-called thin-layer cascades (TLCs) benefits from the advantages of open systems – direct sun irradiance, cooling by evaporation, simple cleaning and maintenance, and efficient degassing. They also profit from several features usually associated with closed systems, such as the operation at high cell densities combined with high biomass productivity and harvesting efficiency. Nevertheless, large-scale cultivation in open units can suffer from some natural and technological perturbations [2]. As the production is scaled up, the control of algal growth becomes more complex and requires the regulation of several interconnected culture variables to achieve optimum values. Among them, irradiance, temperature, supply of nutrients, pH, and dissolved oxygen concentration (DO concentration), particularly when acting in synergy, determine the productivity of the culture [3].

The high ratio of exposed surface to total volume S/V (about 100 m^{-1} and higher) in TLCs results in a very high light supply per unit of culture volume, a feature that increases their volumetric biomass productivity [4], resulting in a high dissolved oxygen accumulation in the culture which can modulate photosynthetic performance of microalgal cultures [5]. Indeed, if the exchange rate of DO with the atmosphere cannot match photosynthetic production, high gradients can develop and have adverse effects on growth/productivity of microalgae cultures due to photoinhibition under high light [6], photorespiration, associated with the oxygenase activity of the Rubisco [7], and oxidative stress [8]. High gradients along the cultivation unit during the day in synergy with high irradiance, can damage the photosynthetic apparatus due to oxidative stress. While there are several reports concerning the effect of high concentrations of oxygen on culture productivity and biomass composition [6], information on the effect of oxygen gradients on photosynthesis in outdoor TLCs is not so common, most likely this is due to the necessity to perform fast measurements to catch warning signals of changes in photosynthesis rates which are not possible using measurements of DO, or chlorophyll. In addition, the variation of dissolved oxygen during cultivation and its relationship with the different steps and pathways of electron transport rate is still unclear [9,10].

Under laboratory conditions the most commonly used measurement of photosynthetic activity in microalgae cultures is the rate of oxygen production [11], this is less so in outdoor conditions [12]. Starting in the 1990s, chlorophyll (Chl) *a* fluorescence techniques were introduced to monitor microalgae mass cultures [13,14]. These techniques assess the photosynthetic efficiency estimating the energy distribution between the photochemical and non-photochemical processes [13,15]. The simultaneous *in-situ* measurement of DO concentration and Chl fluorescence can provide a complete and fast estimate of the physiological status of microalgae at various locations of the cultivation unit. Mathematical modelling can be employed in both *in-situ/ex-situ* measurements of photosynthesis (oxygen production, carbon fixation or electron transport) to predict the growth and productivity of phytoplankton populations as well as microalgae cultures [16]. This idea initiated the establishment of the Group for Aquatic Primary Productivity (GAP). As mentioned in the first GAP publication [17], these workshops emphasize a multi-method approach for monitoring algal photosynthesis which can provide better comparability and reliability of obtained data and its interpretation.

In the presented study, the primary production by the fast-growing *Chlorella vulgaris* strain R-117 was measured outdoors in a thin layer cascade and was characterized by its high growth rate, producing increased DO gradients. The aim of this work was to study the effect of high DO concentration along the TLC on diurnal changes of the photosynthetic performance of the *Chlorella* culture using a multi-technique approach. Photosynthetic activity measurements using *in vivo* Chl *a* fluorescence techniques and oxygen evolution were compared and discussed. A complex set of information has been provided to clarify the response of very dense outdoor cultures to extreme DO gradients.

2. Materials and methods

2.1. Experimental design and culture conditions

Experiments were carried out during the 10th International GAP workshop held at Centre Algatech (GPS coordinates – 48°59′15" N; 14°46′40.630″ E), Institute of Microbiology of the Czech Academy of Science (Třeboň, Czech Republic) in August 2017. A fast-growing strain of *Chlorella vulgaris* strain R117 (*CCALA 1107,* Culture Collection of Autotrophic Organisms, Institute of Botany, Třeboň, Czech Republic) (further as *Chlorella R117*) was used in a one-week trial starting on the 21st of August 2017 (Day 0) between 15:00–16:00 h to avoid photostress. During the trial the weather conditions were fair, with stable light conditions and no rainfall, although the first three mornings were cold (6–10 °C).

For the trial, an outdoor culture was diluted 10 times with a mineral medium as described previously [13]. The culture was grown in a 90-m^2 TLC with a total volume of 600 L (Fig. 1A). The mean thickness of the culture layer was 6 mm which determined the surface-to-total-volume ratio (S/V) of about 150 m^{-1}. The culture was circulated by a centrifugal pump, which provided a flow speed of about 32 $m^3 h^{-1}$, and a linear speed of 0.5 m s^{-1} on a flat surface with a 0.5% slope. The microalgae culture was pumped from a retention tank and evenly distributed at the high point of an upper cultivation plane, flowed down along the surface of the upper platform to a trough, which transferred the suspension to the top of the lower platform. From the end of the lower plane, the suspension passed through a net (to enhance the efficiency of the oxygen degassing) and into the retention tank located under the unit. CO_2 was supplied on demand (pH stat) in the tubing before the pump. The culture flow was usually stopped at the end of the day (19:00 h) and collected in the retention tank, where it was maintained suspended by compressed air bubbling until the next morning. The culture exposure on the cascade surface only begun once the ambient temperature increased to 15 °C (usually about 07:00 h, but occasionally 08:30–09:00 h) to avoid photoinhibition at low temperature. Samples were taken at certain locations on the TLC (Fig. 1A) at certain times during the day (8:30 to 17:00 h), 21 to 26 August 2017.

2.2. Determination of dry weight and Chl content

Biomass dry weight (DW) was measured by filtering 5 mL of culture samples on pre-weighed glass microfiber filters (GC-50). The filters with the cells were washed twice with deionized water (approximately 50 mL total), oven-dried at 105 °C for 8 h, and then transferred to a desiccator to equilibrate to laboratory temperature and weighed (precision ±0.01 mg). Daily biomass productivity (g DW L^{-1} d^{-1}) was calculated as the difference in DW biomass concentration between two consecutive days. Total biomass productivity (g DW L^{-1} d^{-1}) was calculated as the difference in biomass concentration between initial and final days.

For the Chl assay, 500 μL samples were collected in 2 mL Eppendorf tubes and centrifuged at 13,000 rpm for 3 min (centrifuge Minispin, Eppendorf). The pellet was suspended in 500 μL of 100% methanol, the tubes were put into a laboratory ultrasound bath for 2 min, then cooled down in an ice bath and centrifuged at 10,000 rpm for 1 min. If necessary, the extraction was repeated several times until the pellet was colourless. The absorbance of the combined supernatants from all extraction steps was measured at 665 and 750 nm using a high-resolution spectrophotometer (UV 2600 UV-VIS, Shimadzu, Japan; slit width of 0.5 nm) and the concentrations of pigments were calculated according to Wellburn [18]. Dry weight and pigment assays were carried out in triplicate.

2.3. In-situ measurement of physico-chemical variables

The following physico-chemical parameters were measured using portable multiparameter instrument (Hanna®), temperature, pH, and DO concentration. The rate of oxygen production (RO_2) was calculated according to Doucha and Lívanský [19]:

(i) The build-up of DO concentration was estimated between the initial (P1) and final (P5) (distance of 25.7 m) sampling points of the cascade (Fig. 1A). The net rate of oxygen production by the microalgae culture was calculated from the gradient in DO concentration between these two points, taking into account the mass transfer of oxygen between the suspension and the atmosphere, concerning water temperature and an average estimate of turbulence, using the following formula:

$$R_{O_2,DOmean} = \left(\frac{uh}{L}\right)\left(C_{O_2,L} - C_{O_2,0}\right) + K_{L,O_2}\left(C_{O_2,mean} - C_{O_2}{}^*\right) \quad (1)$$

where $R_{O_2,DOmean}$ = mean rate of photosynthetic oxygen production in 1 m^2 of culture area (g O_2 m^{-2} h^{-1}); u = velocity of the flow of suspension flow on the culture area (m h^{-1}); h = thickness of the suspension layer on the culture area (m); L = distance between the DO concentration measurement points (m); $C_{O_2,L}$ and $C_{O_2,0}$, = DO concentration (g O_2 m^{-3}) at the P5 and P1 sampling points, respectively;K_{L,O_2} = 0.2 (m h^{-1}), mass transfer coefficient for oxygen; $C_{O_2,mean}$ = DO concentration in culture (g O_2 m^{-3});$C_{O_2{}^*}$ = DO concentration in equilibrium with oxygen in ambient atmosphere for each temperature condition (g O_2 m^{-3}). The first part of the equation represents DO concentration increase along the flow path of the culture, and the other expresses mass transfer of oxygen between the culture and the atmosphere, depending on the DO concentration gradient and water temperature.

(ii) An empirical formula that allows us to calculate the rate of oxygen production in the TLC from the light measurements, based on PAR (photosynthetically active radiation) and oxygen production constants with *Chlorella R117* cultures in Třeboň [19], is as follows:

$$R_{O_2,light,mean} = \frac{k\,I_0}{(K_I + I_0)} \quad (2)$$

where$R_{O_2,light,mean}$ = mean rate of oxygen evolution by microalgae referred to 1 m^2 of culture area (g O_2 m^{-2} h^{-1}); k = 12.82 g O_2 m^{-2} h^{-1} (an empirical constant estimated by the curve-fitting in [19]); I_0 = PAR irradiance (μmol photons m^{-2} s^{-1}); light saturation constant K_I = 884 μmol photons m^{-2} s^{-1} (PAR).

2.4. Ex-situ oxygen production measurements

Rates of photosynthetic oxygen evolution as a function of irradiance (P-E curve) and dark respiration were measured in samples taken from the outdoor TLC at certain times (8:30, 14:00 and 17:00 h). A Clark-type oxygen sensor was mounted in a closed temperature-controlled (30 °C) and stirred chamber (DW2/2, Hansatech Instrument Ltd., Norfolk, UK) connected to a control box (Oxygraph Plus, Hansatech, King's Lynn, England). Diluted microalgae samples (2 mL) (~ 4 μg Chl mL^{-1}) were used. A series of stepwise increasing light irradiance levels (white LED light source, 0–2000 μmol photons m^{-2} s^{-1}) was applied at 1 min intervals and the oxygen evolution [μmol O_2 mg Chl^{-1} h^{-1}] was recorded using the OxyTrace+ software (Hansatech Instrument Ltd., Norfolk, UK). The measurements were recorded in triplicate. Equation of Eilers and Peeters [20] were used to fit P-E curves and calculate the variables described above (RO_{2max}, α, E_k and E_{opt}).

2.5. Bio-optical light absorption measurements

In vivo Chl spectral absorption cross-section of the microalgal cells was measured according to Shibata et al. [21] by a double-beam spectrophotometer (Shimadzu UV-3000) using 1cm cuvettes. It was carried out in samples collected at four times points (8:30, 11:00, 14:00 and 17:00 h) and diluted with fresh medium to obtain an optical density between 0.1 and 0.8. To minimize the impact of the light scattering effect from the cell surface, the sample cuvette was placed close to the detector window of the photomultiplier and a light diffusor was placed between it and the cuvette. Specific absorption cross-sections of the suspension [$a_{sus(\lambda)}$, m^{-1}] were calculated from the spectral absorption measurements (400–750 nm):

$$a_{sus(\lambda)} = 2.303 * OD_{sus(\lambda)} * 100 \quad (3)$$

where $OD_{sus(\lambda)}$ is the optical density of the suspension at a determined wavelength (a value at 750 nm was subtracted), 2.303 is the conversion

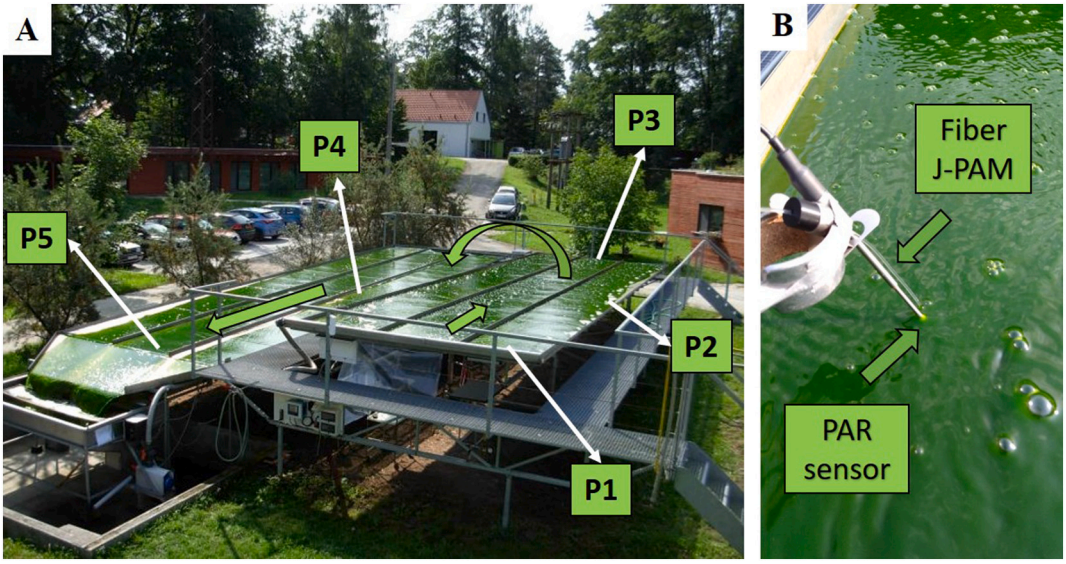

Fig. 1. Thin-layer Cascade (TLC). (A) Cultivation unit with sampling points: P1 = output of culture – start (0 m length of flow), P2 = middle of the upper platform (6.4 m distance from the start), P3 = end of the upper platform (12.8 m length of flow), P4 = middle of lower platform (19.2 m length of flow), P5 = end of the lower platform (25.6 m length of flow). (B) Detail of the light sensor and fibreoptics used for *in-situ* continuous monitoring of the *in vivo* chlorophyll *a* fluorescence. The fiberoptics of the fluorimeter Junior-PAM (Walz GmbH, Effeltrich, Germany) and the spherical PAR sensor (US-SQS, Walz GmbH, Effeltrich, Germany) were submerged directly into the microalgal culture.

factor from $\log_{10}$ to ln, and 100 is the conversion from cm to m. Chl-specific absorption cross-section [a^*, m^2 mg^{-1} Chl] was calculated by dividing a by the Chl concentration expressed in mg m^{-3}. The absorptance [As, r.u.] in the PAR range was calculated from the spectral absorption measurements (400–750 nm):

$$As = 1 - 10^{-OD_{(\lambda)}} \quad (4)$$

2.6. *In vivo* Chl *a* fluorescence measurements

Two *in vivo* Chl *a* fluorescence techniques were employed to estimate the photosynthetic performance of *Chlorella R117* cultures: fast fluorescence induction kinetics (OJIP-*test*) [22] and saturation pulse analysis of fluorescence quenching to measure quantum yields and the rapid light-response curves (RLCs) [23]. The RLCs can give information on the balance between photochemistry and the Calvin Benson cycle, while the OJIP-test provides information on the redox state of the electron donor-acceptors of the electron transport chain.

2.6.1. *Pulsed amplitude modulation fluorescence*

In vivo Chl *a* fluorescence was determined by Pulse Amplitude Modulated (PAM) fluorimeters *on-line/in situ* in the outdoor cascade units and *off-line/ex situ* in the laboratory using culture samples withdrawn from the unit.

(i) *In-situ* and on-line measurements of fluorescence quenching in the outdoor TLC

The *in situ* measurement of Chl *a* fluorescence in turbulent microalgal cultures is enabled by a fluorescence signal, which is modulated two orders of magnitude faster than the suspension movement in the cultivation unit [13]. The *in vivo* Chl *a* fluorescence in the microalgal culture was recorded during the diurnal cycle at 10 min intervals using Junior-PAM fluorimeter according to Jerez et al. [24]. The optical fibre (100 cm long, 1.5 mm in diameter) and a spherical PAR sensor (US-SQS, Walz GmbH, Effeltrich, Germany), were placed side-by-side in the middle of the upper platform (Fig. 1A, point P2) of the TLC submerged 3 mm deep in the culture (Fig. 1B). Blue light-emitting diodes (LED, 460 nm) were used to apply measuring and saturating light pulses. The winControl-3.2 software was used for data acquisition. The effective quantum yield ($\Delta F'/Fm'$) was calculated as follows:

$$\Delta F'/Fm' = \frac{(Fm' - F')}{Fm'} \quad (5)$$

where F_m' is the maximal fluorescence yield induced by the saturating light pulse and F' is the steady-state fluorescence level measured in the culture adapted to ambient irradiance before the application of saturation pulse. The electron transport rate (ETR) through PSII (μmol electrons m^{-2} s^{-1}) was determined as follows:

$$ETR = \frac{\Delta F'}{Fm'} \times E_{PAR} \times A \times fQA_{PSII} \quad (6)$$

where E_{PAR} is the incident photosynthetically active irradiance (μmol photons m^{-2} s^{-1}), A is the absorptance (dimensionless, Eq. (4)), and fQA_{PSII} is the fraction of incident quanta absorbed by PSII. For *Chlorophyceae* the value of 0.51 was determined by Johnsen & Sakshaug [25]. ETR was converted to oxygen production rate $R_{O_2,fluo}$ (μmol O_2 m^{-2} h^{-1}) using the equation:

$$R_{O2,fluo} = ETR \times QR \times 3600 \quad (7)$$

where QR is the quantum requirement for oxygen production (1 mol O_2/5 mol photons by PSII [26]) and the factor of 3600 converts seconds to hours.

(ii) *Ex situ* (laboratory) measurements of Rapid Light Curves (RLC).

Dark-adapted samples (10 min, in triplicate) were exposed to a series of stepwise increasing irradiance intensities using two types of PAM-fluorimeters: PAM-2500 (red light) and Junior-PAM (blue light) as to compare both measurements. The F_0 (basal fluorescence from fully oxidized reaction centres of PSII) and F_m (maximal fluorescence level from fully reduced PSII reaction centre), were determined in the dark-adapted samples to obtain the maximal PSII quantum yield (F_v/Fm) where F_v is the difference between F_m and F_0 [27].

RLCs measured by PAM-2500 were determined in a 2 mL sample (3–4 μg Chl mL^{-1}) placed in a light-protected chamber while mixing (liquid-phase DW2/2,Hansatech) thermostated at 30 °C. A series of stepwise increasing light irradiances (red LEDs, 0–55–120-184-383-580-1232-1850 μmol m^{-2} s^{-1}) were automatically applied at 20 s intervals to obtain the light-adapted fluorescence level F′ (fluorescence yield in the light), and at the end of each step a saturating pulse (>10,000 μmol photons m^{-2} s^{-1}, 0.6 s duration) was triggered to reach the maximum fluorescence level F_m' (maximum fluorescence in the light). The RLCs using Junior-PAM were performed in a light-protected measuring chamber (15 mL) with 20 s of exposure to the twelve irradiance intensities (Blue LEDs; 0–25–45-66-90-125-190-285-420-625-845-1150-1500 μmol photons m^2 s^{-1}) of actinic light, obtaining the light-adapted fluorescence level F′ and the maximum fluorescence level F_m'at the end of each step using the saturating pulse.

The actual PSII photochemical quantum yield in the light ($\Delta F'/Fm'$) was calculated as $(F_m' - F')/Fm'$ at a particular irradiance level. ETR per Chl unit (ETR*) was calculated as follows [μmol electrons mg Chl $^{-1}$ s^{-1}]:

$$ETR^* = \frac{\Delta F'}{Fm'} \times E_{PAR} \times a^* \times fQA_{PSII} \quad (8)$$

where a^* is the Chl-specific absorption cross-sections (m^2 mg^{-1} Chl). Then, ETR* *vs* irradiance were plotted to obtain the photosynthesis-irradiance (P-E) curves and these were fitted by non-linear least-squares regression using the tangential function reported by Eilers and Peeters [20] to estimate variables as maximum electron transport rate (ETR_{max}), the initial slope of the curve (α) as an estimate of photosynthetic efficiency, the onset of photosynthesis saturating irradiance (E_k) and the onset of photoinhibitory irradiance (E_{opt}). Non-photochemical quenching [NPQ = (F_m - F_m')/F_m'] of the fluorescence is a measure of energy dissipation by regulated and non-regulated quenching mechanisms. NPQ is considered an indicator of photoprotection to excess irradiance and is inversely related to photochemistry (Y(II)) [15].

2.7. *Fast fluorescence induction kinetics (OJIP curves)*

Fast Chl fluorescence induction kinetics (OJIP curves) were measured *ex-situ* using a handheld fluorimeter (AquaPen AP-100, P.S.I. Ltd., Czech Republic) adapted for liquid samples. The OJIP measurements were carried out in diluted samples (0.2–0.3 g DW L^{-1}; 3–4 μg Chl mL^{-1}), in a 3-mL measuring cuvette (light path of 10 mm) mounted in a light-protected holder in front of the detector (adjustable measuring light pulses, ~ 2.5 μs). Red LEDs served as high-intensity actinic light from both sides of the cuvette (up to 3000 μmol photons m^{-2} s^{-1}), perpendicular to the detector. The OJIP curves were measured in triplicate in the time range between 50 μs and 1 s. The signal rises rapidly from the origin (O) to highest peak (P) *via* two inflections – J and I [28]. The O point (50 μs) of the fluorescence induction curve represents a minimum value (designated as constant fluorescence yield F_0) when PQ electron acceptors (Q_A and Q_B) of the PSII complex are oxidized (open). The inflection J occurs after ~2–3 ms of illumination and reflects the dynamic equilibrium (quasi steady-state) between Q_A and Q_A^-. The J–I phase (at 30–50 ms) corresponds to the closure of the remaining reaction centres, and the I—P (ending at about 300–500 ms) corresponds to a full reduction of the plastoquinone pool (equivalent to maximum fluorescence level Fm) [29]. The samples were taken from points P1 to P5

(Fig. 1A) and immediately exposed to OJIP-test *in-situ* to avoid having to transfer samples to the laboratory, corresponding to the effective quantum yield of PSII photochemistry in light-adapted culture samples. At the same time, a parallel series of samples were incubated in the dark for 10 min and then OJIP-curves were recorded, corresponding to the maximum quantum yield of PSII photochemistry in dark-adapted culture samples.

Several performance indexes (PIs) have been defined, which should provide information on the structure and function of PSII, as well as on the efficiency of specific electron transport reactions in the thylakoid membrane, and they were proposed to quantify microalgae tolerance to stress according to Stirbet et al. [22]. In a large number of photosynthetic studies, the variable F_v/F_m have been as a stress indicator, however other authors [22,30–33] have proposed another more responsive variable, called the performance index (PI). In this work, the total performance index on absorption basis ($PI_{ABS,\ TOTAL}$) was used, which is related to the functioning of the whole linear electron transport showing both positive or negative values, as negative values expressa "loss" of ability for energy conservation [22].

$PI_{ABS,\ TOTAL}$ is calculated from four components as follows:

$$PI_{ABS,TOTAL} = (RC/ABS)x\left[\frac{(TR_0/ABS)}{(1-TR_0/ABS)}\right]x\left[\frac{(ET_0/TR_0)}{(1-ET_0/TR_0)}\right]x\left[\frac{(RE_0/ET_0)}{(1-RE_0/ET_0)}\right] \quad (9)$$

The four components used in the formula are:

RC/ABS – the ratio of the total number of active PSII reaction centres (RC) per absorption flux (ABS) as estimated from (Fv/Fm)/(Mo/Vj);
TR_0/ABS – the maximum quantum yield of PSII photochemistry that leads to Q_A reduction per absorption flux (ABS), corresponding to Fv/Fm;
ET_0/TR_0 – the efficiency with which a trapped exciton by the PSII reaction centre leads to electron transfer (E_0) from Q_A^- to plastoquinone (PQ) estimated as (Fm-Fj)/Fv;
RE_0/ET_0 – the efficiency of the electron transport from plastoquinol (PQH_2) in the PQ pool, to the final electron acceptors of PSI estimated as (Fm-Fi)/(Fm-Fj);

where F_0=$F_{0.05ms}$; Fj = F_{2ms}; Fi = F_{30ms}; Fm = fluorescence maximum; Mo/Vj = 4 ms^{-1} ($F_{0.3ms}$-$F_{0.05ms}$)/(F_{2ms}-$F_{0.05ms}$).

$log(PI_{ABS,TOTAL})$ is calculated as follows:

$$log\left(PI_{ABS,TOTAL}\right) = log(RC/ABS) + log\left[\frac{(TR_0/ABS)}{(1-TR_0/ABS)}\right] + log\left[\frac{(ET_0/TR_0)}{(1-ET_0/TR_0)}\right] + log\left[\frac{(RE_0/ET_0)}{(1-RE_0/ET_0)}\right] \quad (10)$$

2.8. Statistical analyses

Descriptive statistics (average and standard deviation) were used to analyse the data. Statistical differences were tested by one-way ANOVA using the R software. *A posteriori* comparison was made using Tukey's test ($\alpha = 0.05$). When the data did not adjust to a normal distribution and homogeneity of variance assumptions, statistical differences were tested by one-way ANOVA permutation test using the R.

3. Results and discussion

The effect of DO concentration on the photosynthetic performance was evaluated by monitoring oxygen production and *in vivo* Chl *a* fluorescence measurements. One approach was to monitor *in vivo* Chl *a* fluorescence *on-line/in-situ* during the diel cycle to estimate the actual photosynthetic activity and the other was to measure *ex-situ* using dark-adapted samples collected at certain time periods from the outdoor culture unit [34]. Then, both approaches can be correlated to get the complex set of information. During the first three days (days 1–3) of the trial, morning temperatures ranged between 6 and 10 °C and the maximal midday values within 20–29 °C. The culture was placed on the TLC at about 08:30–09:00 h to avoid photoinhibition due to the synergism of high irradiance and low culture temperature. On days 4–5 morning temperatures ranged between 14 and 15 °C (at midday between 30 and 34 °C) and the culture was placed on the TLC around 08:00 h. The irradiance on day 2 to day 5 was adequate to support high growth as the midday maxima ranged between 1200 and 1800 μmol photons m^{-2} s^{-1}, respectively, while on day 0 and day 1 irradiance was lower, or variable, but still rather fair (data not shown).

3.1. In-situ estimation of oxygen production and electron transport rate

The rate of oxygen production (R_{O_2}) of culture as function of time was estimated using two methods, *i.e.*, from the *in situ* DO concentration measurements ($R_{O_2,DOmean}$) (Eq. (1)) according to Doucha and Lívanský [19]; and using the effective fluorescence quantum yield measured by *in-situ* monitoring ($R_{O_2,fluo}$) (Eq. (7)) (Fig. 2). The rate of DO production, $R_{O_2,DOmean}$, ranged from 2 to 3 in the morning to 8–10 g O_2 m^{-2} h^{-1} at midday. As expected, oxygen evolution increased during the day and dropped during the afternoon and night. The$R_{O_2,fluo}$ showed a similar daylight-dependent pattern but lower values in the morning than those of $R_{O_2,DOmean}$ (Fig. 2A). The estimation of oxygen production provided by both *in-situ* methods showed a good correlation and similar absolute values, thus validating the use of *on-line in situ* fluorescence monitoring technique to asses DO production rate. The rate of oxygen production $R_{O_2,DOmean}$ normalized on the basis of both Chl (μmol O_2 mg Chl^{-1} h^{-1}) and biomass (mg O_2 g^{-1} DW h^{-1}) decreased in the course of the trial (Fig. 2B and C), probably due to an increasing self-shading and the consequent photolimitation of the culture, when its biomass density increased 6-fold, from 3 to 18 g DW L^{-1}, from day 1 to day 5, respectively).

The rate of oxygen production per Chl (Fig. 2B) was greater in the morning compared to the afternoon values during the previous day (similar Chl concentration, mg L^{-1}), most likely as result of the photosystems recovery at night. The highest O_2 production rate normalized to Chl and biomass was found on days 1–2 (Fig. 2B and C), when biomass density was 3 to 8 g DW L^{-1}, while the overal DO production rate per unit area remained stable from day to day. The reported values of oxygen production per biomass (mg O_2 g DW^{-1} h^{-1}, Fig. 2C) are in accordance with those measured for cells acclimated to the low light

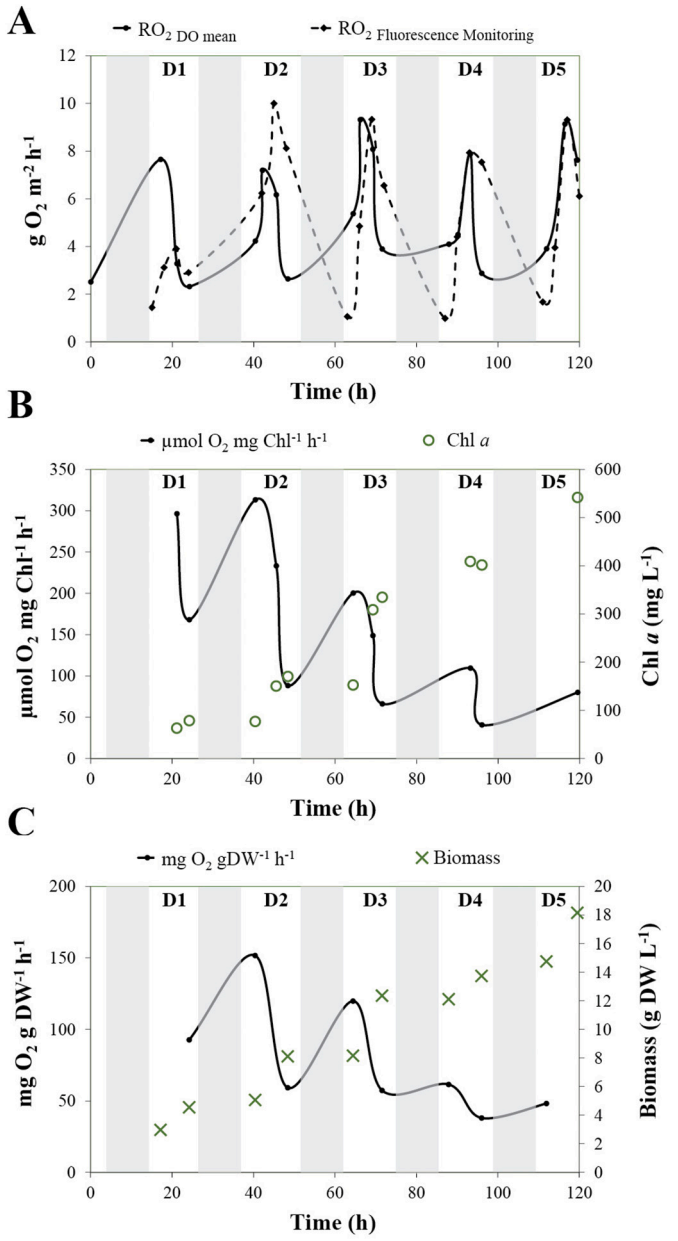

Fig. 2. Rate of oxygen production (RO_2) calculated during cultivation trial of *Chlorella* R117 from *in situ* measurements in TLC. (A) Rate of O_2 production expressed as RO_2 (g O_2 m^{-2} h^{-1}) estimated from ΔDO concentration ($RO_{2,\ DOmean}$; solid line) and fluorescence monitoring ($RO_{2\ Fluorescence\ Monitoring}$; dotted line). (B) Oxygen production calculated per Chl *a* unit (µmol O_2 mg Chl^{-1} h^{-1}). (C) Oxygen production calculated per biomass unit (mg O_2 g^{-1} DW h^{-1}). Grey areas indicate darkness periods (night). D1-D5 = day 1 to day 5.

intensity that is usually found in dense cultures [35,36]. The mean rate of oxygen evolution ($R_{O_2,DOmean}$, g O_2 m^{-2} h^{-1}) of the culture expressed on an areal basis was hyperbolically dependent on ambient irradiance (Fig. 3), similarly to the P-E curves. The data showed correlation with the fitted curves using the light-dependence semi-empirical model (Eq. (2)) proposed by Doucha and Lívanský [19], both using the empirical variables as well as those obtained from fitting of the experimental data. These results allowed the validation of the semi-empirical model proposed by Doucha and Lívanský. The measured R_{O_2} values were in the range from 2 to 10 g O_2 m^{-2} h^{-1} corresponding to values reported by several authors [19,37,38].

Chl fluorescence has been considered a reliable and sensitive technique to monitor the photosynthetic activity and consequently

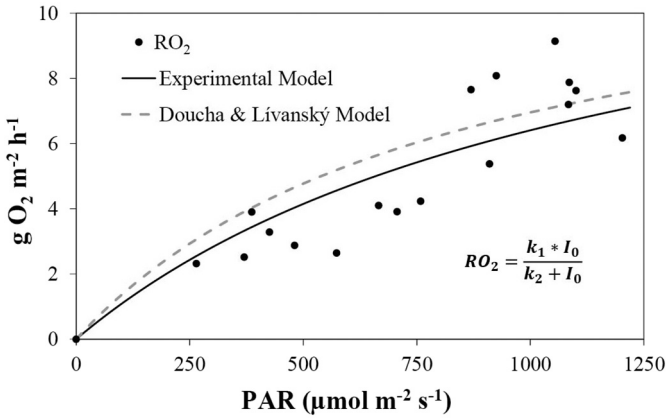

Fig. 3. The rate of oxygen production ($RO_{2,DOmean}$; g O_2 m^{-2} h^{-1}) calculated as a function of ambient irradiance. (PAR, µmol photons m^{-2} s^{-1}) The RO_2 (black circles) correspond to data recorded throughout the 5-day trial outdoor. The models of RO_2 as function of ambient irradiance correspond to the model (grey dashed line) published by Doucha & Lívanský (2006) and to the model variables fitted by the experimental data (black solid line).

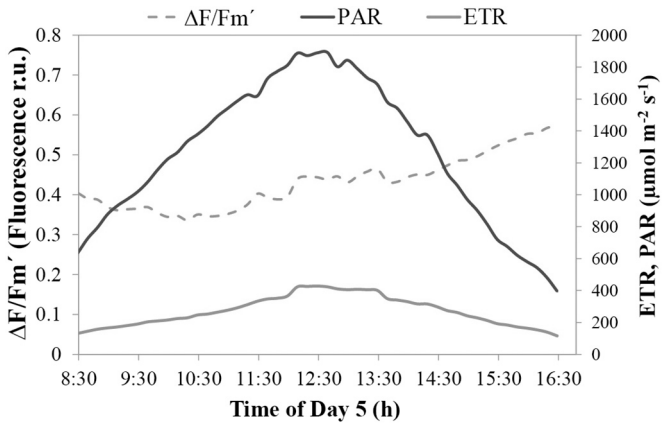

Fig. 4. On-line monitoring fluorescence (using Junior-PAM) recorded *in-situ* at 10-min intervals during day 5 in the *Chlorella* R117 culture grown in thin-layer cascade. Diurnal change of ΔF′/Fm′ (grey dashed line, [Fluorescence r.u.]), PAR (black solid line, [µmol photons m^{-2} s^{-1}]) and electron transport rate, ETR, (grey solid line, [µmol electrons m^{-2} s^{-1}]) are shown. Biomass concentration was as in Fig. 2C.

physiological status and growth of microalgae cultures [24,34]. The diel course of *on-line/in-situ* monitoring of *in vivo* Chl *a* fluorescence showed a slight decrease of $\Delta F'/F_m'$ in the morning and then a continuous increase in the afternoon (Fig. 4), but not the commonly seen down-regulation (*e.g.* photoinhibition) of photosynthesis at midday due to high irradiance. On the contrary, several authors have observed a decrease of ΔF′/Fm′ at midday as expected for a high-irradiance impairment of electron transport capacities beyond Q_A [24,39,40]. Only on days 1 to 3, when the culture was still not as dense, a slight decrease of Fv/Fm (measured *off-situ* in dark adapted samples) was observed at midday (data not shown). Toward day 5, as the biomass density increased, the midday depression in Fv/Fm diminished, probably due to an acclimation of the culture to lower average irradiance per cell, until its total fading on day 5. *In situ* photosynthetic activity was estimated as the electron transport rate (ETR, Eq. (6)) using the actual photochemical yield ΔF′/Fm' and PAR data, and *off-situ* measurements of the culture absorptance in the culture samples taken at 8:30, 11:00, 14:00 and 17:00 h. The course of ETR corresponded to that of ambient irradiance and indicated their interrelation (Fig. 4).

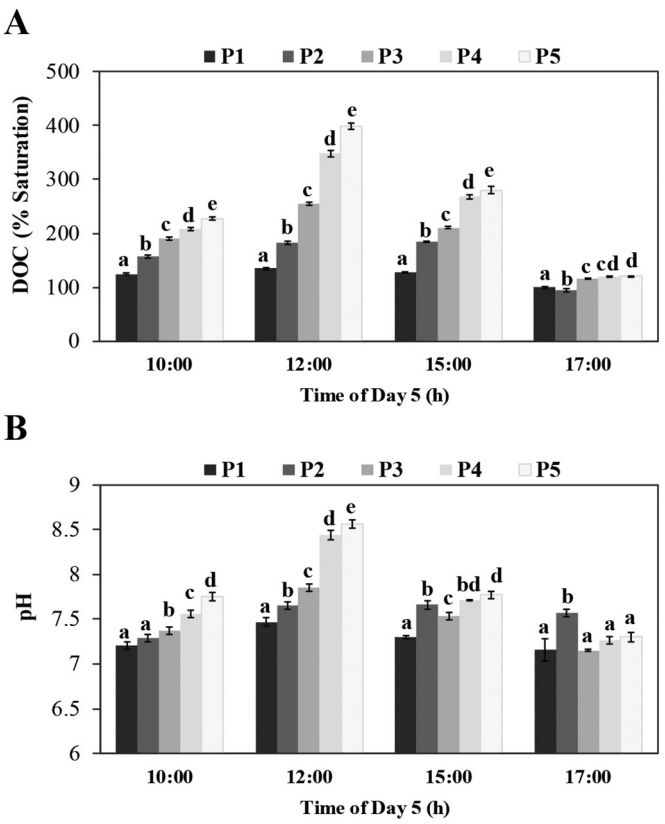

Fig. 5. Values of dissolved oxygen concentration (DO concentration) expressed as % of saturation (A) and pH (B) in outdoor *Chlorella* R117 culture grown in thin-layer cascade during day 5 at various measuring points (P1 to P5 measured in triplicate; see legend of Fig. 1). Biomass concentration was as in Fig. 2C.

3.2. *Effect of DO concentration gradients on photosynthetic electron transport in outdoor cultures*

On day 5 both daily values of DO (% saturation) and pH monitored at various positions along the TLC lane increased from P1 to P5 (Fig. 5). It indicated a high photosynthetic activity by culture volume unit, leading to the accumulation of DO and CO_2 uptake downstream along the cascade. The highest gradient of DO concentration (ΔDO concentration) between the start (P1) and end of the cultivation area (P5) was found at 12:00 h, reaching 3 times higher DO concentration at P5 (398% sat., *i.e.*, about 31 mg O_2 L^{-1}) than that found at P1 (135% sat.). Apparently, due to the high photosynthetic activity of high-density culture, the rate of oxygen production exceeded the rate of oxygen diffusion to the environment *via* the liquid/air interface, despite the high surface to volume ratio in this TLC (S/V ratio of ~150 m^{-1}). Although an efficient degassing was achieved in the retention tank, as at the start of cultivation surface the DO concentration decreased to about 120% Sat, the high oxygen gradient observed in the final part of cultivation area (points P4 and P5) could affect the photosynthetic rate. For example, in the present trials oxygen saturation of 124–135% was recorded at the beginning of the cultivation area of TLC between 10:00 and 12:00 h which corresponded to the effective quantum yield of PSII, $\Delta F'/F_m'$ between 0.62 and 0.55 (Fig. 6). The effect of the DO concentration was more significant when measured in the middle and at the end of the cultivation area and was found to be 190–255% (P3 at 10:00 and 12:00 h respectively) and 227–398%85 (P5 at 10:00 and 12:00 h respectively) of DO concentration, which corresponded to a $\Delta F'/F_m'$ between 0.55–0.40 and 0.42–0.34 respectively. The course of both variables was antiparallel – the higher the DO gradient the lower $\Delta F'/F_m'$. As the culture was circulated faster, the photochemical activity of the culture quickly recovered to the values close to 0.6 which is physiological when the DO concentration decreased below 200%.

A significant reduction in the photosynthetic activity above 200% DO saturation was also observed in cultures of *Scenedemus almeriensis,* [12,35]. Likewise, a 30% loss in biomass productivity of a *C. vulgaris* culture was found at DO concentration over 30 mg L^{-1} [6]. A reduction of the growth rate was observed in a *Spirulina* culture grown under high DO concentrations of about 300% Sat [44]. Similarly, an increase in the oxygen concentration from 100 to 400% Sat reduced the growth rate of *Neochloris oleoabundans* to one half when cultured under higher irradiance (500 μmol photons m^{-2} s^{-1}) and by 23% under lower irradiance (200 μmol photons m^{-2} s^{-1}) [41]. These impacts of DO oversaturation could be a result of photoinactivation. In this case, it might be more appropriate to speak about 'down-regulation' of photosynthetic activity since the damage to the photosynthetic apparatus is regulatory *via* some protective mechanisms as the culture activity at the start after degassing is recovered (Fig. 6). At high DO concentrations, photorespiration might be induced due to oxygenase activity of Rubisco, reducing carbohydrate synthesis and enhancing the synthesis of phosphoglycolate [42]. Despite the high values of DO concentration observed downstream in the TLC, the flow was so fast, that the culture was exposed to high DO concentration only briefly (~25 s between the points P3 and P5), and it occurred only around midday. In addition, in such dense cultures (>15 g DW L^{-1}) average cell irradiance in the intermittent light regime (the light/dark cycles of about 0.5 s; [13]) was probably acting against the

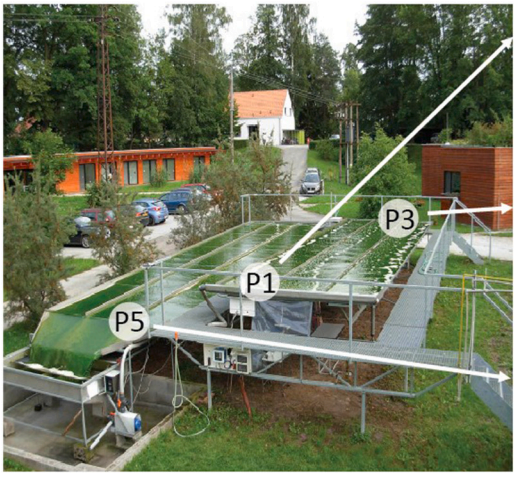

P1	10:00h	12:00h
ΔF´/Fm	0.62 ± 0.09	0.55 ± 0.04
DO %	124 ± 1,8	135 ± 2.0

P3	10:00h	12:00h
ΔF´/Fm	0.55 ± 0.05	0.40 ± 0.06
DO %	190 ± 2.8	255 ± 3.8

P5	10:00h	12:00h
ΔF´/Fm	0.42 ± 0.05	0.34 ± 0.06
DO %	227 ± 3.3	398 ± 5.9

Fig. 6. Monitoring points of dissolved oxygen concentrations (DO %) and the effective quantum yield $\Delta F'/F_m'$ in the thin-layer cascade. The data were measured at 10:00 and 12:00 h on day 5.

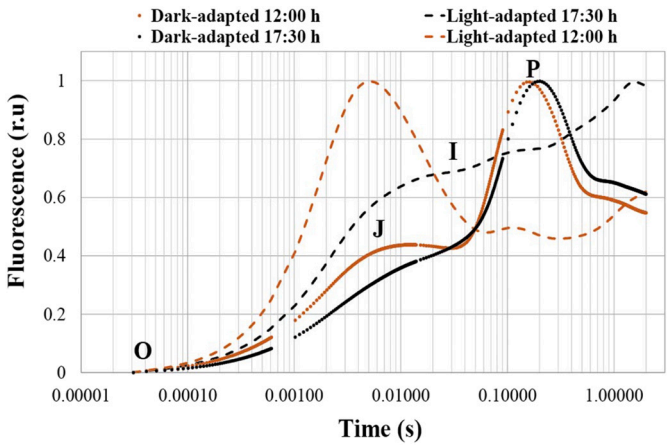

Fig. 7. OJIP curves of dark-adapted (10 min) and light-adapted samples taken from outdoor *Chlorella* R117 culture at 12:00 h and late afternoon 17:30 h of day 5. Data are the means of samples P1 to P5 measured in triplicate. Biomass concentration was as in Fig. 2C.

triple photoinhibitory synergism of high irradiance *vs* high DO concentration *vs* time of exposure.

Fast Chl fluorescence induction kinetics (OJIP test) was determined for both light-adapted and dark-adapted samples, to examine changes in their photosynthetic performance at different positions in the TLC unit throughout the day. OJIP kinetics in the TLC unit (average data from samples taken in the connecting trough) were measured at low (17:30 h) and high (12:00 h) irradiances in both light-adapted (immediately after sampling) and dark-adapted samples (10 min) (Fig. 7). The curves' shapes indicate a large adaptation-dependent difference in the status of the photosynthetic apparatus [43]. The dark-adapted samples showed the classical shape of the OJIP curve, with distinct J inflection and maximum at the point P, while the light-adapted samples revealed a change in the maximal fluorescence depending on the daytime. At midday the kinetics showed a large peak in the J inflection, which reflects the accumulation of the reduced primary acceptor of PSII (Q_A^-) due to high irradiance exposure, indicating a slow-down of electron transport rate at the acceptor side of the PSII complex [18,24,50]. As expected, the fluorescence yield in the initial inflection points (J-I) was higher in the light-adapted samples than in the dark-adapted samples, as more electron acceptors were reduced by light exposure at midday (Fig. 7).

The performance index on absorption basis ($logPI_{ABS,TOTAL}$, which is related to the function of the whole linear electron transport) of light-adapted samples decreased along the culture flow in correlation with the increasing DO concentration (Fig. 8). The drop in $logPI_{ABS,TOTAL}$ along the TLC was greater at 15:00 h (Fig. 8C) as compared with earlier daytimes, although both irradiance and oxygen gradient exposure were not at maximum values (Figs. 5A and 8B). Therefore, this could be the result of the accumulated constraints on the photosynthetic performance due to numerous short-time exposure to high DO gradients during the preceding hours. The OJIP results obtained with dark-adapted samples did not show differences between the sampling points (P1-P5) (data not shown), indicating that the effect of short-time DO concentration gradient and high light exposure is the result of a down regulation of PSII that is reversible by a 10 min dark incubation.

The decrease of $logPI_{ABS,TOTAL}$ in the light adapted samples (which was calculated for the four components, see Section 2.7 and Eq. (10)) at 15:00 h was reflected in about 38% lower values (ANOVA $p < 0.05$) of the RC/ABS variable (the ratio of total number of active PSII reaction centres per absorption flux) and ET_0/TR_0 (efficiency with which a trapped exciton by PSII reaction centre leads to electron transfer from Q_A^- to plastoquinone) between P1 and P4 (data not shown). TR_0/ABS (quantum yield of PSII photochemistry that leads to Q_A reduction, Y(II)

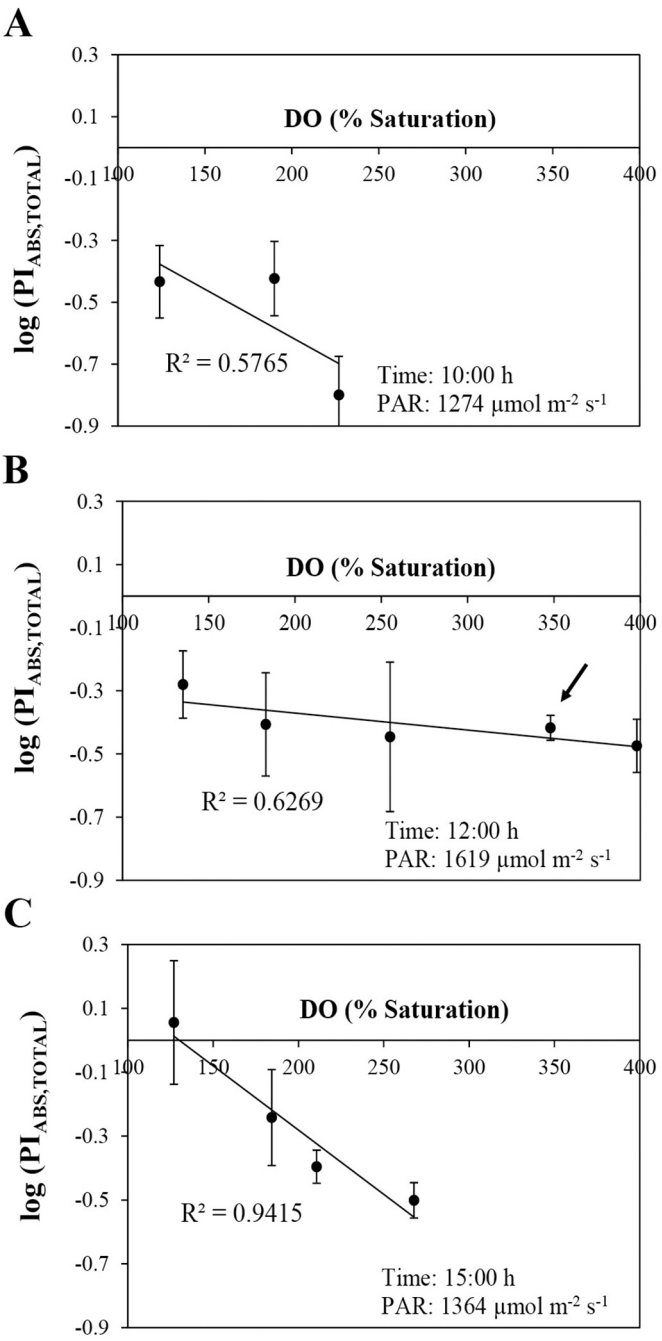

Fig. 8. Diurnal variations in the total performance index, calculated on absorption basis ($logPI_{ABS,TOTAL}$) from fast fluorescence induction kinetics measurements (OJIP curves) as a function of dissolved oxygen concentration (DO % saturation) in light-adapted samples on day 5 at 10:00 h (A), 12:00 h (B), 15:00 (C), and 17:30 h (D). Each point corresponds to the different positions in the thin-layer cascade unit (P1-P5 measured in triplicate, see Fig. 1). Biomass concentration was as in Fig. 2C.

in light adapted samples) did not show significant differences between P1 and P4. On the contrary, RE_0/ET_0 (efficiency of the electron transport from the PQ pool to the final electron acceptors of PSI) revealed a 196% increase (ANOVA $p < 0.01$) between P1 and P4 (data not shown). This increase could be explained by a regulatory role of the Mehler reaction that enhances the re-oxidation of the PQ pool by electron transfer to O_2 at the reducing side of PSI [9,45]; and the decrease of RC/ABS by an increase of the reduction state of electron acceptors at PSII side during light exposition from P1 to P5. At midday the $logPI_{ABS,TOTAL}$ showed a

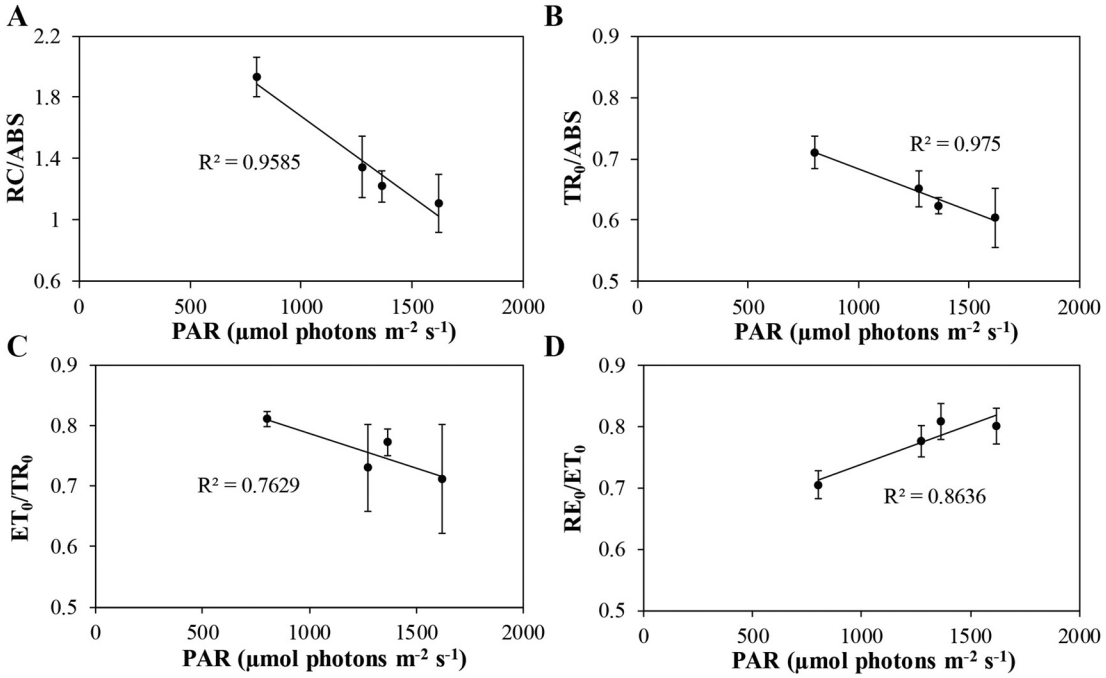

Fig. 9. Photochemical variables calculated from fast fluorescence induction kinetics (OJIP curves) of dark-adapted samples on day 5 as a function of outdoor irradiance. Data are the means of samples P1 to P5 measured in triplicate for each daytime sampling. (A) The ratio of total number of active PSII reaction centres per absorption flux (RC/ABS). (B) Maximum quantum yield of PSII photochemistry that leads to Q_A reduction (TR_0/ABS = Fv/Fm). (C) The efficiency with which a trapped exciton in PSII reaction centre leads to electron transfer from Q_A^- to PQ (ET_0/TR_0). (D) The efficiency of the electron transport from plastoquinol (PQH_2) in the PQ pool, to the final electron acceptors of PSI (RE_0/ET_0).

slight recovery after flow of the culture through the channel connecting upper and lower lanes of the TLC (arrow), where the microalgal cells were less illuminated due to the greater depth of the culture in that section (Fig. 8B). The recovery after the connection trough was principally expressed by an increase in RC/ABS, TR_0/ABS and ET_0/TR_0 values (data not shown). Therefore, the connection channel could help the re-oxidation of the electron acceptors from the PSII side at high irradiance.

The photochemical data obtained from the OJIP measurements with dark-adapted samples were plotted against ambient irradiance obtained throughout the day (Fig. 9, each point is the average of samples P1 to P5 taken at 10:00, 12:00, 15:00 and 17:00 h). The variables RC/ABS (Fig. 9A), TR_0/ABS (Fig. 9B), and ET_0/TR_0 (Fig. 9C) decreased as a function of ambient irradiance which turned in a 45% decrease of the $PI_{ABS,TOTAL}$ (ANOVA $p < 0.05$). RE_0/ET_0 increased as a function of irradiance, thereby implying an increase in efficiency of the electron transport from the PQ pool to the final electron acceptors of PSI (Fig. 9D). This could support the hypothesis of the activation of the regulatory role of the Mehler reaction [9,45], since the numerous exposures of culture to high oxygen gradients throughout the cultivation period could induce changes and adaptations of the photosynthetic apparatus for counterbalancing of abiotic stress. These mechanisms would be overstimulated at high irradiance to deal with the excess electron flow and the limitation of CO_2-assimilation under photorespiration. Photorespiration could serve as an energy sink, preventing the over-reduction of the electron transport chain, especially under stress conditions [46]. The PSI acceptor side is the place where some abiotic stresses can modify the capacity to generate ATP and NADPH, by redirecting electrons toward alternative electron sinks [9]. Nevertheless, precise information about the mechanism of the alternative electron sinks and its importance in the regulation of photosynthesis is not definite, so that the hypotheses about the mechanism proposed require more experimental evidence [46–48]. Several methodological approximations for the study of the energy fluxes around both photosystems and alternative electron sinks appear in studies that used 77 K measurements [49], DUAL-PAM fluorimeter (Y_{PSI} and Y_{PSII}) [50], Fast Repetition Rate Fluorescence (FRRF) [26], and electrochromic shift of photosynthesis pigments [51].

The decrease of RC/ABS, TR_0/ABS and ET_0/TR_0 as a function of irradiance (reduction by about 30%*, 8%* and 10% between the minimum and maximum irradiance values, respectively, ANOVA *$p < 0.001$) confirm the inactivation of a fraction of PSII reaction centres (lower RC/ABS values) (Fig. 9), as this would diminish the electron donation capacity of the PSII reaction centres to Q_A (lower TR_0/ABS) and PQ-pool (lower ET_0/TR_0) reduction [29]. A similar trend of RC/ABS and the increasing irradiance suggesting a faster disassembling rate of reaction centres compared to the antenna was also found by Solovchenko et al. [52]. However, it is likely that the limited light penetration into the culture would be insufficient to generate a significant photodamage to the photosynthetic apparatus. Therefore, the down-regulation of the donor side of PSII would have a similar effect on the fluorescence variables observed here. There are various metabolic processes that can down-regulate the PSII activity. The effect of the Mehler reaction on the down-regulation of PSII quantum yield is indicated by an increase in transmembrane ΔpH; and it might be responsible for most of the non-photochemical quenching (NPQ) developed when CO_2-assimilation is limited [53]. State transitions (1→2), LHCII phosphorylation and migration of a fraction of the antennae to the PSI by lateral diffusion in the thylakoids [45] could represent another process that slow down the reduction PSII electron acceptors and increase the electron transfer around PSI [29,54] as can be deduced by the increase in RE_0/ET_0. In addition, two aspects should be considered about the interpretation of OJIP results: one aspect is the dark-relaxation halftime of state transitions process (2→1), which takes around 8–10 min but it may vary among species [55] (10 min dark adaptation were used in this work); the second aspect is that the state transition may become the major component of fluorescence quenching in light-limited conditions as in high-density cultures [55].

OJIP-test evaluates the performance of relatively fast photosynthetic processes (one-second), therefore, results of oxygen production measurements and *in vivo* Chl fluorescence measured over a longer timeline

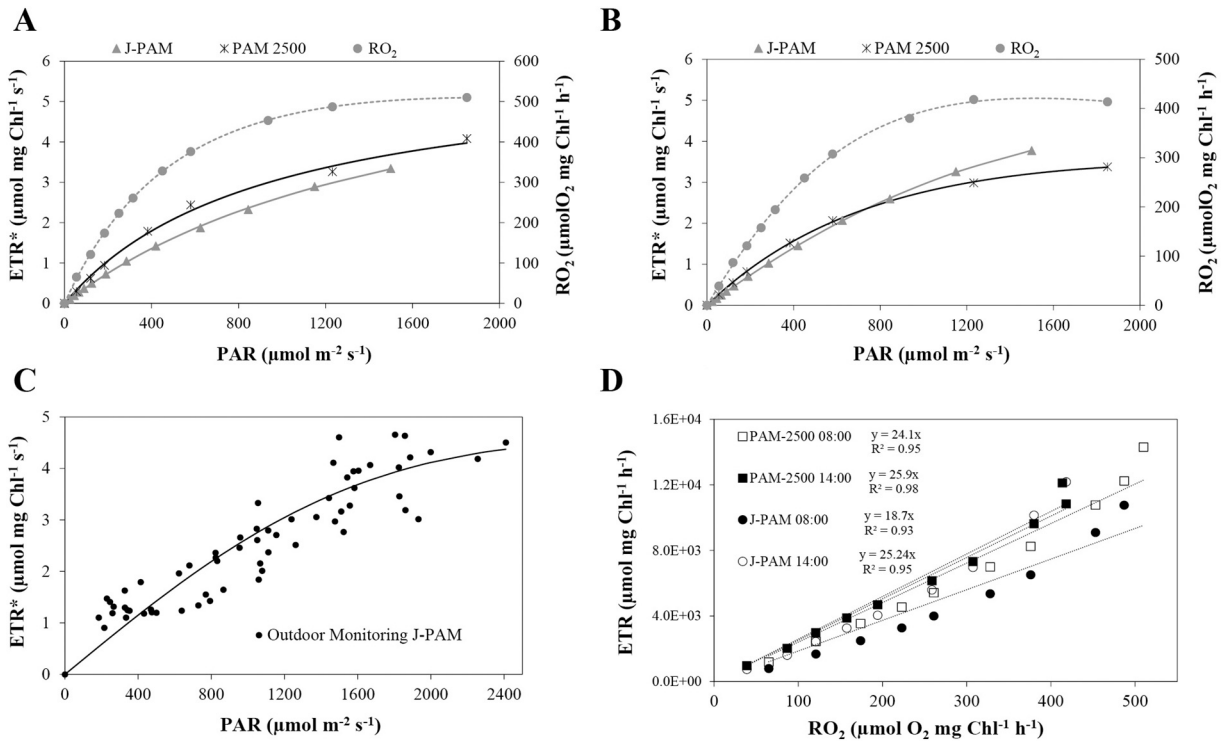

Fig. 10. The rate of oxygen production (RO_2, [µmol O_2 mg Chl^{-1} h^{-1}]) and electron transport rate per unit of Chl (ETR*, [µmol electrons mg Chl^{-1} s^{-1}]) was calculated as a function of irradiance from off-line/*ex situ* measurements in samples taken from outdoor TLC on day 5 at 8:30 h (A) and at 14:00 h (B). Three techniques were used for estimation of P-E curves: rapid light curves (RLC) by PAM method using two type of devices, PAM-2500 (black crosses) and Junior-PAM (grey triangles); and steady-state light response curve of oxygen production (circles). (C) ETR* curve was estimated from outdoor ΔF′/Fm′ and ambient PAR monitoring data measured *in situ* using the Junior-PAM fluorimeter and from Chl-specific absorption cross-sections measured along the day. (D) Correlation of ETR* [µmol electrons mg Chl^{-1} h^{-1}] and oxygen production (µmol O_2 mg Chl^{-1} h^{-1}) measured off-line/*ex situ* in samples taken from the outdoor TLC on day 5 at 8:30 h and at 14:00 h.

Table 1
Comparison of P-E curve variables fitted according to the Eilers and Peeters (1988) tangent model using fluorescence-based and oxygen-based measurements. Off-line and *ex-situ* results correspond to the rapid light-response curves (RLCs) performed with PAM-2500 and Junior-PAM fluorimeters. *Ex-situ* steady state curves of photosynthetic oxygen evolution were performed using a Clark-type oxygen electrode (Oxylab+, Hansatech). Solar ETR curve performed with Junior-PAM on-line and *in situ* measurements of Y(II) and ambient PAR. Variables: α = photosynthetic efficiency; R_{O_2max} = maximum oxygen production [µmol O_2 mg $(Chl)^{-1}$ h^{-1}]; ETR^*_{max} = maximum electron transport rate per unit of Chl *a* [µmol electrons mg $(Chl)^{-1}$ s^{-1}]; E_k = onset of light saturation (µmol photons m^{-2} s^{-1}); Fv/Fm = maximum quantum yield of PSII photochemistry; NPQ_{max} = maximum non-photochemical quenching.

Methods	Time	α	ETRmax - RO_2max	E_k	Fv/Fm	NPQmax	r^2
PAM 2500	08:30 h	0.006	5.98	942.3	0.72	0.26	0.9976
	14:00 h	0.005	3.47	677.9	0.75	0.45	0.9999
J-PAM	08:30 h	0.004	6.44	1542.3	0.59	0.20	0.9998
	14:00 h	0.004	4.65	1213.9	0.56	0.19	0.9999
Solar ETR curve J-PAM		0.003	4.51	1541.1	nd	nd	0.8381
O_2 Evolution	08:30 h	1.2	509.8	426.5	nd	nd	0.9999
	14:00 h	0.7	420.8	580.3	nd	nd	0.9997

(P-E curves) were used to analyse the complete time scale of photosynthesis [22].

3.3. *Ex-situ* estimations of rapid and steady-state light response curves

Rapid light-response curves (RLCs) of *in vivo* Chl *a* fluorescence, steady-state light response curves (SS-LRCs) of oxygen production, and outdoor measurements (ETR recorded *in situ vs* PAR irradiance) are presented in Fig. 10. The variables estimated from the light-response curves (α, ETR^*_{max} and R_{O_2max}) showed a decrease in all *ex-situ* measurements at 14:00 h compared to 08:30 h (Table 1). These results correlated with the higher values of irradiance, temperature and DO concentration (Figs. 4 and 5) in the culture at midday. Several authors reported a reduction of photosynthetic activity and biomass production under such conditions due to photorespiration and the onset of photostress [6,8,35,39,41,56]. An over-reduction of PSII transporters (as observed in Fig. 7 at midday) could give an explanation for the lower values of photosynthetic activity at 14:00 h. The photosynthetic ETR saturated at a higher irradiance (E_k) than that which saturated oxygen evolution (Table 1), a difference that can result from the impact of the aforementioned alternative electron sinks, which would lead to a net reduction of O_2 production while maintaining the electron transport. In photosynthetic studies, the variable F_v/F_m is used as a stress indicator [49]. In the present study, however, this variable did not follow oxygen evolution, *i.e.*, it did not show an afternoon depression at 14:00 h (Table 1), indicating that the photsynthetic apparatus suffered little or no damage. Another indicator of the photosynthetic activity is the capacity of energy dissipation considered as photoprotection mechanism, in this case NPQ related to the thermal dissipation *via* the xanthophyll cycle [57–59]. The culture showed low values of NPQ at both time

periods (Table 1), an observation that would suggest an acclimation by the microalgae to the low light availability inside the culture.

The oxygen production measured *in situ* and calculated according to Doucha and Lívanský [5] (Fig. 2B, day 5) at 11:00 h [80 μmol O_2 mg $(Chl)^{-1}$ $h^{-1;}$ at 1100 μmol photons m^{-2} s^{-1}] was significantly lower than the estimated from photosynthesis light-response curves [418 μmol O_2 mg (Chl) $^{-1}$ h^{-1} at 1232 μmol photons m^{-2} s^{-1}; Fig. 10B]. This can be expected for a dense culture with photolimitation. Therefore, *in-situ* oxygen production per Chl unit was lower than *ex-situ* oxygen production at the same incident irradiance.

A linear relation between ETR and oxygen evolution was observed for the whole irradiance interval applied for each device, except for the last point of RLCs (Fig. 10D), similar to [11,60] but unlike [60–62] depending on the species and culture conditions. According to Figueroa et al. [61] and Gilbert et al. [60] the conversion of fluorescence based electron transfer rates through PSII into oxygen production is a reliable procedure for light intensities below the saturation level. As light intensities approach saturation, the correlation between ETR and oxygen production deviate from linearity due to physiological regulation processes (*i.e.* electron cyclic flow around PSII, Mehler reaction, photorespiration, increase of oxygen uptake due to increased mitochondrial activity) [9,60]. The quantum yield of PSII in this study was calculated to be at the range of about 19–26 $\mu mol_{electrons}/\mu mol_{O2}$ (the slope of linear regression in Fig. 10D). These values correspond well with those reported by Costache et al. [35], of between 22 and 35 $\mu mol_{electrons}/\mu mol_{O2}$ for several species of green microalgae. Higher values than 4 (theoretical value for PSII) in the ratio of ETR and photosynthesis as C fixation (C^{14}) were measured in natural phytoplankton communities at natural marine locations [63]. Electron and oxygen consuming processes can explain the higher values than theoretical which is in agreement with results obtained by Blache et al. [11]. Other electron sinks that are not used for C-fixation are cyclic electron transport around PSI, nitrogen and sulphur assimilation that also consume ATP and NADPH and the export of reducing equivalents to mitochondria or peroxisomes [49]. In addition, in green microalgae, PAM fluorescence measurements assume an equal distribution of absorbed photons to PSII and PSI, but changes in the functional absorption cross section at PSII (*e.g.* changes of transition state) and optical absorption cross-section measurements can affect the results ([σ_{PSII}] *e.g.* in ref. [64]).

The RLCs variables obtained by fluorescence measurements showed similar behaviour between the two fluorimeters (Table 1). Nevertheless, J-PAM revealed higher values of the ETR^*_{max} compared to PAM-2500 data (Table 1). The differences observed between both types of fluorimeters may be the low maximum irradiance for actinic light of J-PAM (1500 μmol photons m^{-2} s^{-1}), which was below the plateau of the P-E curve (Fig. 10). This could lead to an overestimation ETR^*_{max} and underestimation of NPQ that was calculated by extrapolation of the P-E model [20]. In addition, the two instruments used light sources of different colours (that are absorbed and impact photosynthesis differently in green algae), J-PAM with blue light and PAM-2500 with red light. Interestingly, solar P-E curve performed by *on-line/in situ* fluorescence measurements throughout the day showed similar results with curves obtained by off-line/*ex situ* RLCs fluorescence-based measurements with the same device model, validating the methodology under our experimental conditions (Table 1). In contrast, other authors showed different values of rETR measured *in-situ* compared to those measured *ex-situ* [24,44]. Nevertheless, Jeréz et al. [24] observed a linear correlation between both measurements (*in situ* and *ex situ*). The usefulness of *in-situ* monitoring is that, in contrast to *ex situ* measurements, it is carried out under actual culture conditions, *i.e.* irradiance, temperature, DO concentration, pH, and mixing rate. Another advantage is the possibility to obtain a continuous stream of data and thereby following the physiological state of the culture in real time, *in-situ* and on line. Such data are useful for develop models to control microalgae production units.

4. Conclusions

A spectrum of *in-situ* and *ex-situ* photosynthesis monitoring techniques was applied simultaneously to examine the photosynthetic performance of the highly productive culture of *Chlorella* R117 grown outdoors in thin-layer cultivation cascades. During the diel cycle the culture experienced high temporal and spatial gradients in DO concentration along the cultivation area. A certain depression (down-regulation) of photosynthetic activity was observed in some periods of the day (midday) due to the exposure to high DO concentration down the TLC area, but it was quickly reversed when the culture was degassed. The course of the photosynthetic activity and DO concentration was antiparallel – higher for the former and the lower in the latter. High DO gradients are an inevitable consequence of high photosynthetic activity which is – on the other hand – essential for high biomass productivity. Some protective mechanisms, alternative electron sinks and oxygen consuming processes (*e.g.* photorespiration and the Mehler reaction) probably function as no photodamage was observed in these *Chlorella* cultures. This could explain the much higher (than theoretical) ratio between electron transport and oxygen production $\mu mol_{electrons}/\mu mol_{O2}$. *In-situ and ex-situ* fluorescence measurements show some important variables (Fv/Fm, ΔF'/Fm', ETR, OJIP-test) which are useful for the monitoring of photosynthetic performance to optimise outdoor cultures and avoid culture loss in large-scale outdoor microalgae plants.

CRediT authorship contribution statement

Tomás Agustín Rearte: Conceptualization, measurements, data analysis, figure and manuscript preparation. Amir Neori, Paula S.M. Celis-Plá and Félix Álvarez Gómez: Conceptualization, measurements, data analysis, figure and manuscript editing. Jiří Masojídek, Giuseppe Torzillo, Félix López Figueroa and Karolína Ranglová: Team management, planning of experiments, measurements, figure and manuscript editing. Cintia Gómez, Ana Margarita Silva Benavides, Roberto Abdala, Martín Caporgno, Thaís Fávero Massocato, Jaqueline Carmo da Silva, Hafidh Al Mahrouqui, and Richard Atzmüller: measurements and data analysis, figure preparation.

Declaration of competing interest

The authors declare that they do not have any competing financial interests or personal relationships that could influence this manuscript. No conflicts, informed consent, or human or animal rights are applicable to this study.

Acknowledgements

This work was funded by National Sustainability Programme I of The Ministry of Education, Youth and Sports of the Czech Republic (project Algatech Plus LO1416) and in part by the EU programme Horizon 2020 (project SABANA, grant no. 727874) and Interreg Czech Republic-Austria programme (project Algenetics ATCZ15). TAR was supported by the Universidad de Buenos Aires, Argentina. FLF thanks Junta de Andalucía for financial support of the research group "Photobiology and biotechnology of aquatic organisms" (FYBOA-RNM295). PCP was supported by the Santander scholarship to young research and project FONDECYT No 11180197. AN thanks BARD Research Grant Award No. US – 4599-13R (The United States – Israel Binational Agricultural Research and Development Fund) and additional funds from the Israeli Ministry for Science and Technology and the Dead Sea-Arava Science Center (DSASC) to AN.

References

[1] T. Grivalský, K. Ranglová, J.A. Manoel Câmara, G.E. Lakatos, R. Lhotský, J. Masojídek, Development of thin-layer cascades for microalgae cultivation : milestones (review), Folia Microbiol. (Praha). 64 (2019) 603–614.

[2] H. Chang, Y. Zou, R. Hu, H. Feng, H. Wu, N. Zhong, J. Hu, Membrane applications for microbial energy conversion: a review, Environ. Chem. Lett. 18 (2020) 1581–1592, https://doi.org/10.1007/s10311-020-01032-7.

[3] I. Rawat, R. Ranjith Kumar, T. Mutanda, F. Bux, Biodiesel from microalgae: a critical evaluation from laboratory to large scale production, Appl. Energy 103 (2013) 444–467, https://doi.org/10.1016/j.apenergy.2012.10.004.

[4] J. Masojídek, M. Sergejevová, J.R. Malapascua, J. Kopecký, Thin-layer systems for mass cultivation of microalgae: flat panels and sloping cascades, in: Algal Biorefineries, 2015: pp. 1–557. doi:https://doi.org/10.1007/978-3-319-20200-6.

[5] F.G. Acién, E. Molina, A. Reis, G. Torzillo, G.C. Zittelli, C. Sepúlveda, J. Masojídek, Photobioreactors for the production of microalgae (2017), https://doi.org/10.1016/B978-0-08-101023-5.00001-7.

[6] A. Kazbar, G. Cogne, B. Urbain, H. Marec, B. Le-Gouic, J. Tallec, H. Takache, A. Ismail, J. Pruvost, Effect of dissolved oxygen concentration on microalgal culture in photobioreactors, Algal Res. 39 (2019) 101432, https://doi.org/10.1016/j.algal.2019.101432.

[7] S. Raso, B. van Genugten, M. Vermuë, R.H. Wijffels, Effect of oxygen concentration on the growth of *Nannochloropsis* sp. at low light intensity, J. Appl. Phycol. 24 (2012) 863–871. doi:https://doi.org/10.1007/s10811-011-9706-z.

[8] C. Sousa, L. de Winter, M. Janssen, M.H. Vermuë, R.H. Wijffels, Growth of the microalgae *Neochloris oleoabundans* at high partial oxygen pressures and sub-saturating light intensity, Bioresour. Technol. 104 (2012) 565–570, https://doi.org/10.1016/j.biortech.2011.10.048.

[9] P. Cardol, G. Forti, G. Finazzi, Regulation of electron transport in microalgae, Biochim. Biophys. Acta Bioenerg. 1807 (2011) 912–918, https://doi.org/10.1016/j.bbabio.2010.12.004.

[10] W.J. Nawrocki, B. Bailleul, D. Picot, P. Cardol, F. Rappaport, F.A. Wollman, P. Joliot, The mechanism of cyclic electron flow, Biochim. Biophys. Acta Bioenerg. 1860 (2019) 433–438, https://doi.org/10.1016/j.bbabio.2018.12.005.

[11] U. Blache, T. Jakob, W. Su, C. Wilhelm, The impact of cell-specific absorption properties on the correlation of electron transport rates measured by chlorophyll fluorescence and photosynthetic oxygen production in planktonic algae, Plant Physiol. Biochem. 49 (2011) 801–808, https://doi.org/10.1016/j.plaphy.2011.04.010.

[12] M. Barceló-Villalobos, C.G. Serrano, A.S. Zurano, L.A. García, S.E. Maldonado, J. Peña, F.G.A. Fernández, Variations of culture parameters in a pilot-scale thin-layer reactor and their influence on the performance of *Scenedesmus almeriensis* culture, Bioresour. Technol. Reports. 6 (2019) 190–197, https://doi.org/10.1016/j.biteb.2019.03.007.

[13] J. Masojídek, J. Kopecký, L. Giannelli, G. Torzillo, Productivity correlated to photobiochemical performance of *Chlorella* mass cultures grown outdoors in thin-layer cascades, J. Ind. Microbiol. Biotechnol. 38 (2011) 307–317, https://doi.org/10.1007/s10295-010-0774-x.

[14] G. Torzillo, P. Accolla, E. Pinzani, J. Masojidek, In situ monitoring of chlorophyll fluorescence to assess the synergistic effect of low temperature and high irradiance stresses in *Spirulina* cultures grown outdoors in photobioreactors, J. Appl. Phycol. 8 (1996) 283–291.

[15] C. Klughammer, U. Schreiber, Complementary PS II quantum yields calculated from simple fluorescence parameters measured by PAM fluorometry and the Saturation Pulse method, PAM Appl. Notes. (2008) 27–35. doi:citeulike-article-id:6352156.

[16] Q. Béchet, A. Shilton, B. Guieysse, Modeling the effects of light and temperature on algae growth: state of the art and critical assessment for productivity prediction during outdoor cultivation, Biotechnol. Adv. 31 (2013) 1648–1663, https://doi.org/10.1016/j.biotechadv.2013.08.014.

[17] Z. Dubinsky, T. Berman, F. Schanz, Field experiments for in situ measurement of photosynthetic efficiency and quantum yield, J. Plankton Res. 6 (1984) 339–349, https://doi.org/10.1093/plankt/6.2.339.

[18] A.R. Wellburn, The spectral determination of chlorophylls *a* and *b*, as well as total carotenoids, using various solvents with spectrophotometers of different resolution, J. Plant Physiol. 144 (1994) 307–313, https://doi.org/10.1016/S0176-1617(11)81192-2.

[19] J. Doucha, K. Lívanský, Productivity, CO_2/O_2 exchange and hydraulics in outdoor open high density microalgal (*Chlorella* sp.) photobioreactors operated in a Middle and Southern European climate, J. Appl. Phycol. 18 (2006) 811–826. doi:https://doi.org/10.1007/s10811-006-9100-4.

[20] P.H.C. Eilers, J.C.H. Peeters, A model for the relationship between light intensity and the rate of photosynthesis in phytoplankton, Ecol. Model. 42 (1988) 199–215, https://doi.org/10.1016/0304-3800(88)90057-9.

[21] K. Shibata, A.A. Benson, M. Calvin, The absorption spectra of suspensions of living micro-organisms, Biochim. Biophys. Acta 15 (1954) 461–470.

[22] A. Stirbet, D. Lazár, J. Kromdijk, Govindjee, Chlorophyll *a* fluorescence induction: can just a one-second measurement be used to quantify abiotic stress responses? Photosynthetica. 56 (2018) 86–104, https://doi.org/10.1007/s11099-018-0770-3.

[23] U. Schreiber, U. Schliwa, W. Bilger, Continuous recording of photochemical and non-photochemical chlorophyll fluorescence quenching with a new type of modulation fluorometer, Photosynth. Res. 2 (1986) 51–62.

[24] C.G. Jerez, J.R. Malapascua, M. Sergejevová, J. Masojídek, F.L. Figueroa, *Chlorella fusca* (Chlorophyta) grown in thin-layer cascades: estimation of biomass productivity by in-vivo chlorophyll a fluorescence monitoring, Algal Res. 17 (2016) 21–30, https://doi.org/10.1016/j.algal.2016.04.010.

[25] G. Johnsen, E. Sakshaug, Biooptical characteristics of PSII and PSI in 33 species (13 pigment groups) of marine phytoplankton, and the relevance for pulse-amplitude-modulated and fast-repetition-rate fluorometry [1], J. Phycol. 43 (2007) 1236–1251, https://doi.org/10.1111/j.1529-8817.2007.00422.x.

[26] J.C. Kromkamp, N. A. Dijkman, J. Peene, S.G.H. Simis, H.J. Gons, Estimating phytoplankton primary production in Lake IJsselmeer (The Netherlands) using variable fluorescence (PAM-FRRF) and C-uptake techniques, Eur. J. Phycol. 43 (2008) 327–344. doi:https://doi.org/10.1080/09670260802080895.

[27] U. Schreiber, H. Hormann, C. Neubauer, C. Klughammer, Assessment of photosystem II photochemical quantum yield by chlorophyll fluorescence quenching analysis, Aust. J. Plant Physiol. 22 (1995) 209–220.

[28] R.J. Strasser, A. Srivastava, Govindjee, Polyphasic chlorophyll *a* fluorescence transient in plants and cyanobacteria, Photochem. Photobiol. 61 (1995) 32–42, https://doi.org/10.1111/j.1751-1097.1995.tb09240.x.

[29] G. Schansker, S.Z. Tóth, R.J. Strasser, Dark recovery of the Chl a fluorescence transient (OJIP) after light adaptation: the qT-component of non-photochemical quenching is related to an activated photosystem I acceptor side, Biochim. Biophys. Acta Bioenerg. 1757 (2006) 787–797, https://doi.org/10.1016/j.bbabio.2006.04.019.

[30] A. Stirbet, Govindjee, On the relation between the Kautsky effect (chlorophyll *a* fluorescence induction) and photosystem II: basics and applications of the OJIP fluorescence transient, J. Photochem. Photobiol. B Biol. 104 (2011) 236–257, https://doi.org/10.1016/j.jphotobiol.2010.12.010.

[31] A. Srivastava, R.J. Strasser, Govindjee, Greening of peas: parallel measurements of 77 K emission spectra, OJIP chlorophyll a fluorescence transient, period four oscillation of the initial fluorescence level, delayed light emission, and P700, Photosynthetica. 37 (1999) 365–392, https://doi.org/10.1023/A:1007199408689.

[32] R.J. Strasser, A. Srivastava, M. Tsimilli-Michael, The fluorescence transient as a tool to characterize and screen photosynthetic samples, Probing Photosynth. Mech. Regul. Adapt. (2000) 443–480, https://doi.org/10.1016/j.bbabio.2010.10.019.

[33] M. Tsimilli-Michael, R.J. Strasser, In vivo assessment of stress impact on Plant's vitality: Applications in detecting and evaluating the Benefi cial role of Mycorrhization on host plants, in: A. Varma (Ed.), Mycorrhiza. Genet. Mol. Biol. Eco-Function, Biotechnol. Eco-Physiology, Struct. Syst, Third, Springer, 2008, p. 804, https://doi.org/10.1146/annurev.pp.41.060190.000545.

[34] J. Malapascua, C. Jerez, M. Sergejevová, F. Figueroa, J. Masojídek, Photosynthesis monitoring to optimize growth of microalgal mass cultures: application of chlorophyll fluorescence techniques, Aquat. Biol. Environmen (2014) 123–140, https://doi.org/10.3354/ab00597.

[35] T.A. Costache, F.G. Acién Fernández, M.M. Morales, J.M. Fernández-Sevilla, I. Stamatin, E. Molina, Comprehensive model of microalgae photosynthesis rate as a function of culture conditions in photobioreactors, Appl. Microbiol. Biotechnol. 97 (2013) 7627–7637, https://doi.org/10.1007/s00253-013-5035-2.

[36] Y.S. Yun, J.M. Park, Kinetic modeling of the light-dependent photosynthetic activity of the green microalga *Chlorella vulgaris*, Biotechnol. Bioeng. 83 (2003) 303–311, https://doi.org/10.1002/bit.10669.

[37] J. Doucha, F. Straka, K. Lívanský, Utilization of flue gas for cultivation of microalgae (*Chlorella* sp.) in an outdoor open thin-layer photobioreactor, J. Appl. Phycol. 17 (2005) 403–412, https://doi.org/10.1007/s10811-005-8701-7.

[38] K. Lívanský, J. Doucha, CO_2 and O_2 gas exchange in outdoor thin-layer high density microalgal cultures, J. Appl. Phycol. 8 (1996) 353–358.

[39] G. Torzillo, P. Bernardini, J. Masojídek, On-line monitoring of chlorophyll fluorescence to assess the extent of photoinhibition of photosynthesis induced by high oxygen concentration and low temperature and its effect on the productivity of outdoor cultures of *Spirulina platensis* (cyanobacteria), J. Phycol. 34 (1998) 504–510, https://doi.org/10.1046/j.1529-8817.1998.340504.x.

[40] S. Inhken, J. Beardall, J. Kromkamp, C. Gómez Serrano, M. Torres, J. Masojídek, I. Malpartida, R. Abdala, C. Jerez, J. Malapascua, E. Navarro, R. Rico, E. Peralta, J. Ezequiel, F. Figueroa, Light acclimation and pH perturbations affect photosynthetic performance in *Chlorella* mass culture, Aquat. Biol. 22 (2014) 95–110, https://doi.org/10.3354/ab00586.

[41] C. Sousa, A. Compadre, M.H. Vermuë, R.H. Wijffels, Effect of oxygen at low and high light intensities on the growth of *Neochloris oleoabundans*, Algal Res. 2 (2013) 122–126, https://doi.org/10.1016/j.algal.2013.01.007.

[42] T.J. Erb, J. Zarzycki, A short history of RubisCO: the rise and fall of Nature's predominant CO_2 fixing enzyme, Curr. Opin. Biotechnol. 49 (2018) 100–107, https://doi.org/10.1016/j.copbio.2017.07.017.

[43] J.R. Malapascua, K. Ranglová, J. Masojídek, Photosynthesis and growth kinetics of *Chlorella vulgaris* R-117 cultured in an internally LED - illuminated photobioreactor Photosynthetica. 57 (2019) 103–112. doi:10.32615/ps.2019.031.

[44] A.M. Silva Benavides, K. Ranglová, J.R. Malapascua, J. Masojídek, G. Torzillo, Diurnal changes of photosynthesis and growth of *Arthrospira platensis* cultured in a thin-layer cascade and an open pond, Algal Res. 28 (2017) 48–56, https://doi.org/10.1016/j.algal.2017.10.007.

[45] G. Forti, G. Caldiroli, State transitions in *Chlamydomonas reinhardtii*. The role of the Mehler reaction in state 2-to-state 1 transition, Plant Physiol. 137 (2005) 492–499, https://doi.org/10.1104/pp.104.048256.

[46] A. Wingler, P.J. Lea, W.P. Quick, R.C. Leegood, Photorespiration: metabolic pathways and their role in stress protection, Philos. Trans. R. Soc. B Biol. Sci. 355 (2000) 1517–1529, https://doi.org/10.1098/rstb.2000.0712.

[47] M.R. Badger, S. Von Caemmerer, S. Ruuska, H. Nakano, A. Laisk, J.F. Allen, K. Asada, H.C.P. Matthijs, H. Griffiths, Electron flow to oxygen in higher plants and algae: rates and control of direct photoreduction (Mehler reaction) and rubisco oxygenase, Philos. Trans. R. Soc. B Biol. Sci. 355 (2000) 1433–1446, https://doi.org/10.1098/rstb.2000.0704.

[48] A. Vonshak, G. Torzillo, J. Masojidek, S. Boussiba, Sub-optimal morning temperature induces photoinhibition in dense outdoor cultures of the alga *Monodus subterraneus* (Eustigmatophyta), Plant, Cell Environ. 24 (2001) 1113–1118.

[49] H.M. Kalaji, G. Schansker, M. Brestic, F. Bussotti, A. Calatayud, L. Ferroni, V. Goltsev, L. Guidi, A. Jajoo, P. Li, P. Losciale, V.K. Mishra, A.N. Misra, S. G. Nebauer, S. Pancaldi, C. Penella, M. Pollastrini, K. Suresh, E. Tambussi, M. Yanniccari, M. Zivcak, M.D. Cetner, I.A. Samborska, A. Stirbet, K. Olsovska, K. Kunderlikova, H. Shelonzek, S. Rusinowski, W. Bąba, Frequently Asked Questions About Chlorophyll Fluorescence, The Sequel, 2017, https://doi.org/10.1007/s11120-016-0318-y.

[50] A. Sukenik, J. Beardall, J.C. Kromkamp, J. Kopecký, J. Masojídek, S. Van Bergeijk, S. Gabai, E. Shaham, A. Yamshon, Photosynthetic performance of outdoor *Nannochloropsis* mass cultures under a wide range of environmental conditions, Aquat. Microb. Ecol. 56 (2009) 297–308, https://doi.org/10.3354/ame01309.

[51] S. Ferté, L. Guillou, G. Himakawa, A. Krieger-Liszkay, B. Bailleul, Combinig fluorescence and absorption spectrosopy to investigate cyclic electron flow around photosyten I in various microalgae, in: EPC7 7th Eur. Phycol. Congr., 2019: p. 111.

[52] A. Solovchenko, O. Solovchenko, I. Khozin-Goldberg, S. Didi-Cohen, D. Pal, Z. Cohen, S. Boussiba, Probing the effects of high-light stress on pigment and lipid metabolism in nitrogen-starving microalgae by measuring chlorophyll fluorescence transients: studies with a δ5 desaturase mutant of *Parietochloris incisa* (Chlorophyta, Trebouxiophyceae), Algal Res. 2 (2013) 175–182, https://doi.org/10.1016/j.algal.2013.01.010.

[53] U. Schreiber, C. Neubauer, O_2-dependent electron flow, membrane energization and the mechanism of non-photochemical quenching of chlorophyll fluorescence, Photosynth. Res. 25 (1990) 279–293, https://doi.org/10.1007/BF00033169.

[54] B. Demmig-adams, G. Gyozo, W. Adams, Govindjee, Non-photochemical quenching and energy dissipation in plants, Algae and Cyanobacteria, 2014. doi:https://doi.org/10.1007/978-94-017-9032-1.

[55] G. Krause Heinrich, P. Jahns, Non-photochemical energy dissipation determined by chlorophyll fluorescence quenching: characterization and function, in: G.C. Papageorgiou, G. Govindjee (Eds.), Chlorophyll a Fluoresc. A Signat. Photosynth., 2004: pp. 463–495.

[56] C. Sousa, D. Valev, M.H. Vermuë, R.H. Wijffels, Effect of dynamic oxygen concentrations on the growth of *Neochloris oleoabundans* at sub-saturating light conditions, Bioresour. Technol. 142 (2013) 95–100, https://doi.org/10.1016/j.biortech.2013.05.041.

[57] B. Demmig-Adams, Carotenoids and photoprotection in plants: a role for the xanthophyll zeaxanthin, BBA-Bioenergetics 1020 (1990) 1–24, https://doi.org/10.1016/0005-2728(90)90088-L.

[58] J. Serôdio, S. Cruz, S. Vieira, V. Brotas, Non-photochemical quenching of chlorophyll fluorescence and operation of the xanthophyll cycle in estuarine microphytobenthos, J. Exp. Mar. Biol. Ecol. 326 (2005) 157–169, https://doi.org/10.1016/j.jembe.2005.05.011.

[59] D.M. Kramer, J.R. Evans, The importance of energy balance in improving photosynthetic productivity, Plant Physiol. 155 (2011) 70–78, https://doi.org/10.1104/pp.110.166652.

[60] M. Gilbert, C. Wilhelm, M. Richter, Bio-optical modelling of oxygen evolution using in vivo fluorescence: comparison of measured and calculated photosynthesis/irradiance (P-I) curves in four representative phytoplankton species, J. Plant Physiol. 157 (2000) 307–314, https://doi.org/10.1016/S0176-1617(00)80052-8.

[61] F.L. Figueroa, R. Conde-Álvarez, I. Gómez, Relations between electron transport rates determined by plse amplitude modulate cholophyll fluorescence and oxygen evolution in macroalgae under different light conditions, Photosynth. Res. 75 (2003) 259–275.

[62] H. Carr, M. Björk, A methodological comparison of the photosynthetic and estimated electron transport rate in in tropical *Ulva* (Chlorophyceae) species under different light and inorganic carbon conditions, J. Phycol. 39 (2003) 1125–1131.

[63] E. Lawrenz, G. Silsbe, E. Capuzzo, P. Ylöstalo, R.M. Forster, S.G.H. Simis, O. Prášil, J.C. Kromkamp, A.E. Hickman, C.M. Moore, M.-H. Forget, R.J. Geider, D. J. Suggett, Predicting the electron requirement for carbon fixation in seas and oceans, PLoS One 8 (2013), e58137, https://doi.org/10.1371/journal.pone.0058137.

[64] C. Klughammer, U. Schreiber, Apparent PS II absorption cross-section and estimation of mean PAR in optically thin and dense suspensions of *Chlorella*., Photosynth. Res. 123 (2015) 77–92. doi:https://doi.org/10.1007/s11120-014-0040-6.